https://doi.org/10.1016/j.mri.2021.06.005

A Multi-Inversion-Recovery Magnetic Resonance Fingerprinting for Multi-compartment Water Mapping

Di Cui [a †], Edward S. Hui [b], Peng Cao [a*†]

[a] Department of Diagnostic Radiology, The University of Hong Kong, HKSAR, China

[b] Department of Rehabilitation Science, The Hong Kong Polytechnic University, Hong Kong, HKSAR, China

[*] Corresponding to:

Peng Cao

Address: 5 Sassoon Road, Pokfulam, Hong Kong

Email: caopeng1@hku.hk

[†] Authors were contributed equally

Short Running Title: multi-IR MRF

Key words: myelin, brain MRI, multi-contrast MRI, MR fingerprinting

Total Words: 2335

Number of Figures: 6

Introduction

The multiple sclerosis lesion burdens assessment using T2-weighted imaging has been shown to be associated with clinical disability score (1–3). Detection of these lesions based on T1 and T2-weighted as well as fluid-attenuated inversion recovery (FLAIR) images (4,5) could be an indirect way of probing the pathophysiology of the disease. Quantitative analysis of other MRI observable compartments of the water content could also be used to monitor white matter demyelination (6–8) and diagnose and monitor treatment response.

Magnetic resonance fingerprinting (MRF) is a rapid dynamic MRI approach that aims to estimate the MR parameters of biological tissues, which are largely independent of MRI hardware and sequence configurations (9). Previous studies have demonstrated the clinical applications of MRF for brain tumors (10), breast cancer (11), and prostate cancer (12). Considering that brain MRI examination often entails multi-contrast scans, including T1, T2, magnetization transfer, and macromolecule-weightings (e.g., myelin), there is thus an urgent need to extend conventional MRF beyond the estimation of the T1 and T2 of a single brain tissue compartment (12–14). Multi-compartment water mapping by MRI is highly desirable for monitoring demyelination and remyelination processes. Such multi-compartment measurement was conventionally based on the MRI measurement of 16 to 32 echoes to estimate the T2 differences between tissue compartments, namely free water and myelin water (15–17). The myelin water has a significantly shorter T1 and T2 than free water, thereby allowing the myelin water to be distinguished by multi-compartment analysis of MRF data (15–17).

The multi-compartment analysis was a recent breakthrough in MRF (18). It required multiple MRF acquisitions with pseudorandom flip angle schemes at both 1.5T and 3.0T (18). In that study, the estimation of myelin water fraction was demonstrated on 1.5T (18). It is desirable to further extend the application of MRF for multi-compartment analysis. Our study, therefore, aimed to develop a rapid MRF sequence for multi-compartment water mapping. We proposed a multi-inversion-recovery (mIR) MRF method for the estimation of the MR relaxation times of short T1/T2 water in the brain. Our results have demonstrated that this method could achieve a rapid estimation of brain water compartments, which may be useful for the investigation of white matter pathologies such as demyelination.

Methods

Multi-inversion-recovery MRF

All experiments were performed using a 3 T human MRI scanner (Achieva TX, Philips Healthcare) with an 8-channel brain coil for signal reception. An in-house

inversion recovery FISP sequence with variable flip angles (FA) and repetition times (TR) was used for MRF acquisitions (19). A constant angular velocity spiral readout trajectory with an acquisition window of 8.4 ms and a rotation angle of 222.5º after each dynamic was used. Spiral-in/out trajectory was used for a higher signal-to-noise ratio (SNR) while reducing the susceptibility effect (20). The total number of spiral interleaves for full k-space coverage was 144.

Our proposed mIR MRF sequence was sensitized to brain water content that has short T1/T2. The magnetization obtained after repeatedly applying the IR pulse is was specific to the short T1/T2 signals due to the inversion and prolonged recovery of a long T1/T2 signal, as shown in Figures 1 a and b. Other imaging parameters include: 2000 dynamics, 4 IR pulses applied at the 0^{th}, 501^{th}, 1001^{th}, and 1501^{th} TR, constant TR = 10.0 ms for TE = 2 ms or constant TR = 12.5 ms for TE = 6 ms, FA = 0 to 60º (in Fig. 1), TE = 6 ms (for spiral-in/out trajectory) or 2 ms (for spiral-out trajectory), field of view = 300 × 300 mm^2, acquisition matrix = 256 × 256, image resolution = 1.17 × 1.17 mm^2, slice thickness = 5 mm and number of excitation (NEX) = 1. The scan time of mIR MRF was 24 s/slice. Three volunteers were recruited with informed consent. The WOW-180 pulse was used for the inversion (21), and a trapezoid-shaped gradient spoiler was applied with a duration of 0.8 ms and maximum strength of 20.7 mT/m along the z-axis. The image reconstruction was based on a direct non-uniform Fourier transform, and no iterative reconstruction techniques were used. The coil sensitivity was estimated from the sum of coil images from all time points. The coil combination was performed using the sensitivity-weighted sum of all channels of the raw image series.

The mIR MRF acquisition parameters, including the number of IR pulses, the interval between IR pulses, and the readout trajectories (which also coupled with the minimal TE), were also empirically optimized. The mIR enhancement of tissues with short T1/T2 was simulated. We also investigated different readout trajectories for multi-compartment analysis, whereby two separate mIR MRF experiments were performed using spiral-in/out and spiral-in out trajectories in one volunteer.

Multi-compartment analysis

The effects of exchange were ignored in this study. The multi-compartment analysis is was a recent key breakthrough in MRF methodology (18). In our study, we applied this multi-compartment algorithm (18) to our proposed mIR MRF in a pixel-wise fashion. An in-house MATLAB implementation of the non-negative least-square (NNLS) algorithm with a reweighting iteration for updating the joint distribution of the T1/T2 parameter across an imaging slice/volume was implemented (18). The dictionary for mIR MRF was simulated using an extended phase graph method (22,23). Singular value decompression (SVD) was applied to

the dictionary for dimensionality reduction. Singular values/vectors were subsequently thresholded at the 1% of the maximum singular value. The dictionaries after normalization and SVD compression were then used in NNLS analysis. During the NNLS iteration, the myelin compartment was 10 times magnified due to the naturally low concentration, compared with other compartments, i.e., gray matter and white matter free water, as illustrated in Figure 2. We empirically found that this weighting on the short T1/T2 compartment was necessary for the detection of this water compartment. Specifically, an additional compartment type-dependent weighting term was applied to the dictionary elements as shown in Figure 2. We used a 10-time amplification for myelin water to ensure that the peak amplitude of myelin water to be comparable with that of white matter. In addition, we also used the phase of temporally-summed dynamic MRF images as the reference phase to correct the pixel-wise phase variation. After the phase correction, the real part of the MRF signal evolution was used in the reweighted NNLS method. The regularization for L1 norm term for dictionary weighting was 0.5.

In dictionary generation, the T1 and T2 were exponentially distributed, similar to reference (18). The T1 started from a value of 4 s, and multiplied with a decay factor of 0.942 for 100 times, generating values between 3.768 and 0.0102 s. The T2 started from a value of 2 s, and multiplied with a decay factor of 0.91 for 70 times, generating values between 1.82 and 0.0027 s. The range of T1 and T2 for four compartments were $111 \leq T1 \leq 367$ ms and $4 \leq T2 \leq 18$ ms for short T1/T2 water, $1211 \leq T1 \leq 1632$ ms and $46 \leq T2 \leq 189$ ms for GM, $666 \leq T1 \leq 1211$ ms and $35 \leq T2 \leq 74$ ms for WM, and $2336 \leq T1 \leq 3768$ ms and $157 \leq T2 \leq 1820$ ms for cerebrospinal fluid (CSF), respectively. The method achieved maximal spatial separation of compartments as determined empirically from the MRF data in vivo. The spatial separation was the process of finding the boundary between the compartment of interest and the background, e.g., for the gray matter compartment, the white matter and CSF were the background, and the boundary was set so that the background was close to zero. We adjusted the boundaries to achieve “best” separation of different water compartments. The boundaries were estimated based on the T1 and T2 plot, as shown in Figure 3. We checked the T1 and T2 to ensure there was no overlap between different compartments. On images, the wrongly overlapped compartmental images showed scattered or blocky artifacts on top of normal anatomy. After such a process for optimizing the T1/T2 boundaries. We used nearly identical T1/T2 boundaries definition for all experiments.

Results

Our proposed mIR MRF consisted of 4 IRs applied to perturb the signal evolution, thereby allowing differentiation of the short and long T1/T2 components (i.e., blue vs. red curves in Figure 1). Figure 3 shows the MR parametric map of a healthy volunteer's four brain tissue compartments using our proposed mIR MRF. The T1 and T2 water compartments could be rapidly measured using the proposed mIR MRF with a scan time of 24 s/slice. The method achieved maximal spatial separation of compartments, e.g., gray matter and white matter pixels were separated entirely, with T1/T2 ranges determined empirically from the mIR MRF data in vivo.

MRF scans with and without the proposed mIR scheme were compared (Figure 4). The use of mIR scheme improved the detection of short T1/T2 water content. This result was consistent with our simulation in Figure 1 that demonstrated that the mIR scheme created more differences in signal evolutions for short and long T1/T2 compartments. Figure 5 shows the results from mIR MRF acquired with two different spiral readout trajectories, namely spiral-in/out trajectory with TE of 6 ms and spiral-out trajectory with TE of 2 ms, from the same volunteer. The spiral-in/out trajectory provided a higher signal level, compared with the spiral-out trajectory, which was the default trajectory in conventional MRF. The measured signal levels were 0.18 ± 0.09 and 0.16 ± 0.05 for spiral-in/out and spiral-out trajectories in the genu corpus callosum area. The tradeoff was the theoretically lower sensitivity for short T2 components for the spiral-in/out trajectory due to longer TE. Nevertheless, the short T1/T2 water compartment could still be detected with the two spiral trajectories. In Figure 6, as compared to the 4-IR scheme, the short T1/T2 map from the 5-IR scheme showed fewer artifacts, i.e., ringing artifact on the left occipital lobe was minimized by the additional IR pulse.

Discussions

We have demonstrated the estimation of the water compartments of short T1/T2, GM, WM, and CSF, using our proposed mIR MRF. The mIR MRF jointly utilized the T1 and T2 differences of tissue compartments to improve the separation. The proposed mIR scheme showed improvements in the differentiation of short and long T1/T2 compartments, compared with that from MRF without mIR. This is due to the fast recovery of short T1/T2 signal after each IR pulse, compared with that of long T1/T2. As a result, our newly proposed method permits reliable estimation of the brain short T1/T2 or macromolecule-associated content, together with that of the WM and GM.

The spatial location of the short T1/T2 compartment identified using our proposed mIR MRF largely reside within white matter and is consistent with the known

distribution of myelinated axon. The T1 and T2 of this water compartment were smaller than those of white matter (see right panel of Figure 2). The short T1/T2 values of this compartment suggested that it likely originated from the water associated with macromolecule contents, e.g., through magnetization exchange, which might cause a rapid T1 recovery after inversion pulses. The short T2 water compartment could be myelin-associated water, as conventionally probed used multi-echo spin-echo sequence. The literature T2 values for myelin water were ~20 ms at 3T with T1 < 400 ms (24). In the study done by Nagtegaal et. al. (18), myelin water was shown to have $0 < T2 < 40$ ms and $0 < T1 < 200$ ms at 1.5 T. Considering the shorter T2 and longer T1 at the higher field, our reported T1 and T2 ranges, i.e., $111 \leq T1 \leq 367$ ms and $4 \leq T2 \leq 18$ ms, for myelin water were in reasonable agreement with references (18,24). Therefore, this compartment likely corresponds to a weighted combination of short T2 myelin water and magnetization exchange with the myelin-associated macromolecule. We will, therefore, investigate the demyelination/remyelination process in diseases such as multiple sclerosis using mIR MRF in future studies.

We have also compared mIR MRF using a spiral-in/out trajectory with the conventional spiral-out trajectory. The former was known to have a ~40% SNR gain (20) since it measured the k-space twice in each readout. Our results showed that the spiral-in/out trajectory provided a high signal level in short T1/T2 water detection at the expense of signal penalties on the short T2 compartment due to longer TE. To improve the characterization of the short T2 (e.g., < 6 ms) compartment, a dual-echo approach could be used (25). In addition, this dual-echo method can also be extended to the ultrashort echo regime in the future, where the direct measurement of short T1/T2 content could be achieved.

In this study, we have chosen 4-IR for our proposed mIR MRF. To see whether the estimation of short T1/T2 water content would change with the number of IR, we have also performed two separate mIR MRF experiments, one with 4-IR and another with 5-IR. As compared to the 4-IR scheme, the short T1/T2 water map from the 5-IR scheme showed fewer artifacts and improved. This result suggested the need for increasing the number of IR pulses to improve the imaging of short T1/T2 water content.

Exchange effects were ignored in this study, i.e., the model in this study was non-exchange, which might be a source of bias. The B1 inhomogeneity was not considered. The B1 inhomogeneity might have introduced an estimation bias due to its effect on the inversion and excitation pulses. The off-resonance effect was also ignored because of the FISP MRF sequence with gradient spoiler. However, we only considered the non-exchange model with a single frequency component. Therefore, the estimation bias from sequence imperfection might exist in the current study. Correction for B1 inhomogeneity should be considered in future

studies. In addition, we didn't perform the repeatability test in this preliminary study. The reliability of the result will need to be evaluated in a future experiment.

Conclusion

We have successfully developed a new mIR MRF sequence for measuring the brain water compartments, including a short T1/T2 compartment, which likely corresponds to myelin water.

Acknowledgment

This work was supported by Hong Kong HMRF grants 06172916 and 07182706.

Figure Captions

Figure 1 (**a**) The flip angle (FA) and the time point or TR at which inversion pulse (IR) was applied in our proposed multi-inversion-recovery (mIR) MRF sequence. In the current study, an mIR scheme with 4 IR pulses applied every 500 TRs was used. (**b**) MR signal evolution for long (blue) and short (orange) T1 and T2 components. The mIR scheme repeatedly inverses the long T1/T2 compartment signal, thereby enhancing the detection of the short T1/T2 water compartment.

Figure 2 The initialization for the NNLS method, emphasizing on the short T1/T2 compartment. An additional compartment type-dependent weighting term was applied on W_0 for dictionary elements, D. We used a 10-time amplification for myelin water to ensure that the peak amplitude of myelin water to be comparable with that of white matter.

Figure 3 Multi-compartment analysis of our proposed mIR MRF for a healthy volunteer. The scan time was 24s/slice. Four-compartment brain maps were obtained from a direct pixel-wise separation. (left) The first compartment with $111 \leqslant$ T1 $\leqslant 367$ ms and $4 \leqslant$ T2 $\leqslant 18$ ms is considered as short T1/T2 water. (right) the T1/T2 compartments plot. Dash boxes were zoom-in views show the contours of peaks, and the peak amplitudes (as relative abundances) were color-coded. The solid boxes indicate the T1 and T2 ranges for quantifying the different water compartments. It should be noted that the water with short T1/T2 and white matter free water can be separated in the T1/T2 compartments plot. The size of marker indicted the contour of the compartment at the level of amplitude/ relative abundance $\geqslant 1.0$ (in a.u.). For the contour plot, seven levels ranging from relative abundances of 1.0 to 7.0 (in a.u.) were displayed. WM: white matter; GM: grey matter; CSF: cerebrospinal fluid.

Figure 4 Multi-compartment analysis of another healthy volunteer obtained from MRF with and without the proposed mIR scheme. The use of mIR scheme clearly improved the detection of myelin water content. The scan time for both protocols was 24 s/slice.

Figure 5 Multi-compartment analysis of mIR MRF with two different spiral readout trajectories, namely spiral-in/out trajectory with TE of 6 ms and spiral-out trajectory with TE of 2 ms for the same volunteer as that in Figure 3. The spiral-in/out trajectory provided a higher signal compared with the spiral-out trajectory.

Figure 6 The comparison of the short T1/T2 water compartment mapping using our proposed mIR MRF with mIR scheme with 4 versus 5 IR's. Short T1/T2 water content can be detected using either mIR scheme. That from the 5-IR scheme had fewer artifacts.

REFERENCES:

1. Ge Y. Multiple sclerosis: the role of MR imaging. AJNR Am. J. Neuroradiol. 2006;27:1165–1176 doi: 27/6/1165.

2. Lee MA, Smith S, Palace J, Matthews PM. Defining multiple sclerosis disease activity using MRI T2-weighted difference imaging. Brain 1998;121:2095–2102 doi: 10.1093/brain/121.11.2095.

3. Buckle GJ, Gauthier SA, Stankiewicz J, Meier D. Predicting Clinical Progression in Multiple Sclerosis With the Magnetic Resonance Disease Severity Scale. 2008;65:1449–1453.

4. García-Lorenzo D, Francis S, Narayanan S, Arnold DL, Collins DL. Review of automatic segmentation methods of multiple sclerosis white matter lesions on conventional magnetic resonance imaging. Med. Image Anal. 2013;17:1–18 doi: 10.1016/j.media.2012.09.004.

5. Lladó X, Oliver A, Cabezas M, et al. Segmentation of multiple sclerosis lesions in brain MRI: A review of automated approaches. Inf. Sci. (Ny). 2012;186:164–185 doi: 10.1016/j.ins.2011.10.011.

6. Goveas J, O'Dwyer L, Mascalchi M, et al. Diffusion-MRI in neurodegenerative disorders. Magn. Reson. Imaging 2015;33:1491–1499 doi: 10.1016/j.mri.2015.04.006.

7. Christiansen P, Gideon P, Thomsen C, Stubgaard M, Henriksen O, Larsson HBW. Increased water self-diffusion in chronic plaques and in apparently normal white matter in patients with multiple sclerosis. Acta Neurol. Scand. 1993;87:195–199 doi: 10.1111/j.1600-0404.1993.tb04100.x.

8. Horsfield M a, Lai M, Webb SL, et al. Apparent diffusion coefficients in benign and secondary progressive multiple sclerosis by nuclear magnetic resonance. Magn. Reson. Med. 1996;36:393–400 doi: 10.1002/mrm.1910360310.

9. Ma D, Gulani V, Seiberlich N, et al. Magnetic resonance fingerprinting. Nature 2013;495 doi: https://doi.org/10.1038/nature11971.

10. Badve C, Yu A, Dastmalchian S, et al. MR Fingerprinting of Adult Brain Tumors: Initial Experience. Am. J. Neuroradiol. 2017;38:492–499 doi: 10.3174/ajnr.A5035.

11. Chen Y, Panda A, Pahwa S, et al. Three-dimensional MR fingerprinting for quantitative breast imaging. Radiology 2019;290:33–40 doi: 10.1148/radiol.2018180836.

12. Yu AC, Badve C, Ponsky LE, et al. Development of a Combined MR Fingerprinting and Diffusion Examination for Prostate Cancer. Radiology 2017;283:729–738 doi: 10.1148/radiol.2017161599.

13. Kobayashi Y, Terada Y. Diffusion-weighting caused by spoiler gradients in the fast imaging with steady-state precession sequence may lead to inaccurate T 2 measurements in MR fingerprinting. Magn. Reson. Med. Sci. 2019;18:96–104 doi: 10.2463/mrms.tn.2018-0027.

14. Cohen O, Huang S, Mcmahon MT, Rosen MS, Farrar CT. Rapid and quantitative chemical exchange saturation transfer (CEST) imaging with magnetic resonance fingerprinting (MRF). Magn. Reson. Med. 2018:1–15 doi: 10.1002/mrm.27221.

15. Laule C, Vavasour IM, Moore GRW, et al. Water content and myelin water fraction in multiple sclerosis: A T 2 relaxation study. J. Neurol. 2004 doi: 10.1007/s00415-004-0306-6.

16. Du YP, Chu R, Hwang D, et al. Fast multislice mapping of the myelin water fraction using multicompartment analysis of T2* decay at 3T: A preliminary postmortem study. Magn. Reson. Med. 2007 doi: 10.1002/mrm.21409.

17. Laule C, Kozlowski P, Leung E, Li DKB, MacKay AL, Moore GRW. Myelin water imaging of multiple sclerosis at 7 T: Correlations with histopathology. Neuroimage 2008 doi: 10.1016/j.neuroimage.2007.12.008.

18. Nagtegaal M, Koken P, Amthor T, Doneva M. Fast multi-component analysis using a joint sparsity constraint for MR fingerprinting. Magn. Reson. Med. 2019:1–14 doi: 10.1002/mrm.27947.

19. Jiang Y, Ma D, Seiberlich N, Gulani V, Griswold MA. MR fingerprinting using fast imaging with steady state precession (FISP) with spiral readout. Magn. Reson. Med. 2015;74:1621–1631 doi: 10.1002/mrm.25559.

20. Glover GH, Law CS. Spiral-in/out BOLD fMRI for increased SNR and reduced susceptibility artifacts. Magn. Reson. Med. 2001;46:515–522.

21. Murdoch JB, Lent AH, Kritzer MR. Computer-optimized narrowband pulses for multislice imaging. J. Magn. Reson. 1987 doi: 10.1016/0022-2364(87)90336-2.

22. Hennig J. Echoes—how to generate, recognize, use or avoid them in MR-imaging sequences. Part I: Fundamental and not so fundamental properties of spin echoes. Concepts Magn. Reson. 1991 doi: 10.1002/cmr.1820030302.

23. Weigel M. Extended phase graphs: Dephasing, RF pulses, and echoes - Pure and simple. J. Magn. Reson. Imaging 2015;41:266–295 doi: 10.1002/jmri.24619.

24. Lee J, Hyun JW, Lee J, et al. So You Want to Image Myelin Using MRI: An Overview and Practical Guide for Myelin Water Imaging. J. Magn. Reson. Imaging 2021 doi: 10.1002/jmri.27059.

25. Du J, Ma G, Li S, et al. Ultrashort echo time (UTE) magnetic resonance imaging of the short T2 components in white matter of the brain using a clinical 3T scanner. Neuroimage 2014;87:32–41 doi: 10.1016/j.neuroimage.2013.10.053.

Figures

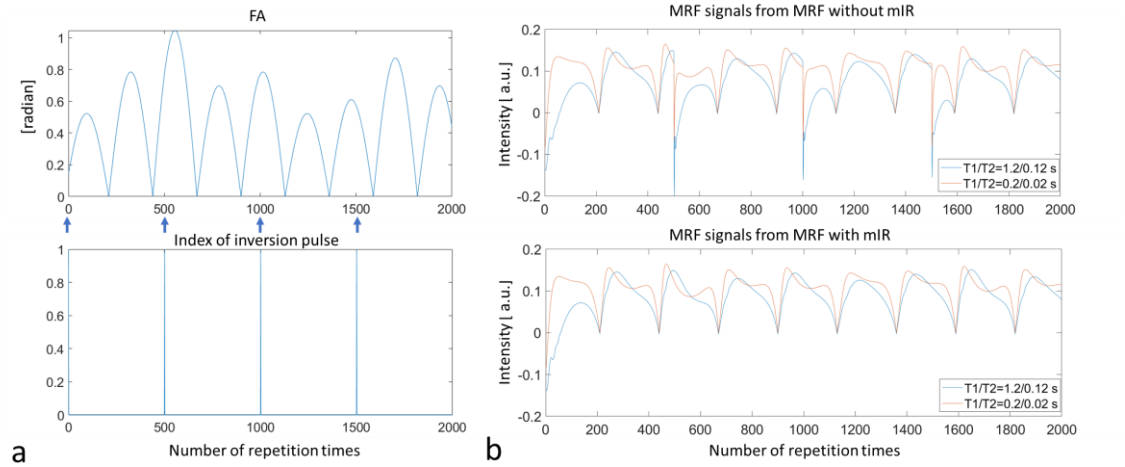

Figure 1 (**a**) The flip angle (FA) and the time point or TR at which inversion pulse (IR) was applied in our proposed multi-inversion-recovery (mIR) MRF sequence. In the current study, an mIR scheme with 4 IR pulses applied every 500 TRs was used. (**b**) MR signal evolution for long (blue) and short (orange) T1 and T2 components. The mIR scheme repeatedly inverses the signal of the long T1/T2

compartment, thereby enhancing the detection of the short T1/T2 water compartment.

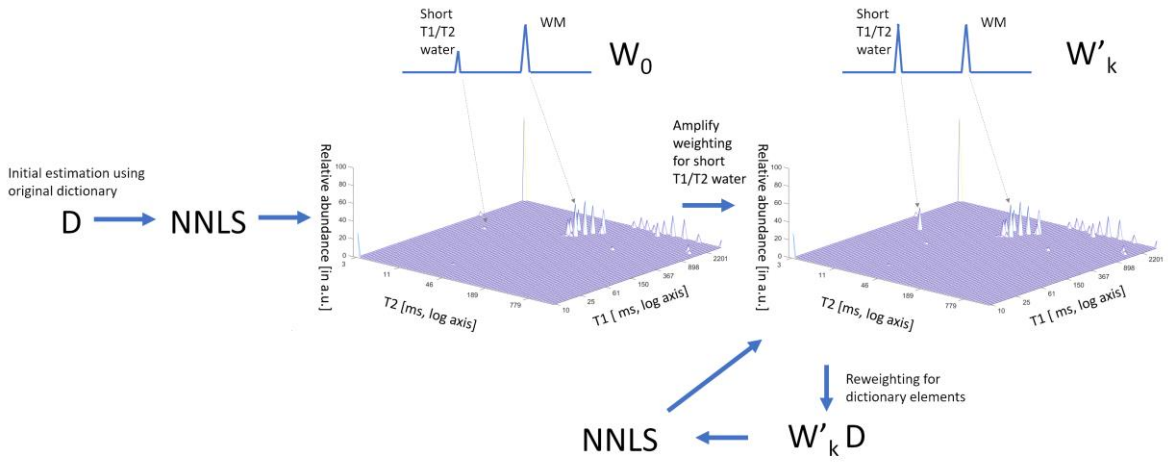

Figure 2 The initialization for the NNLS method, emphasizing on the short T1/T2 compartment. An additional compartment type-dependent weighting term was applied on W_0 for dictionary elements, D. We used a 10-time amplification for myelin water to ensure that the peak amplitude of myelin water to be comparable with that of white matter.

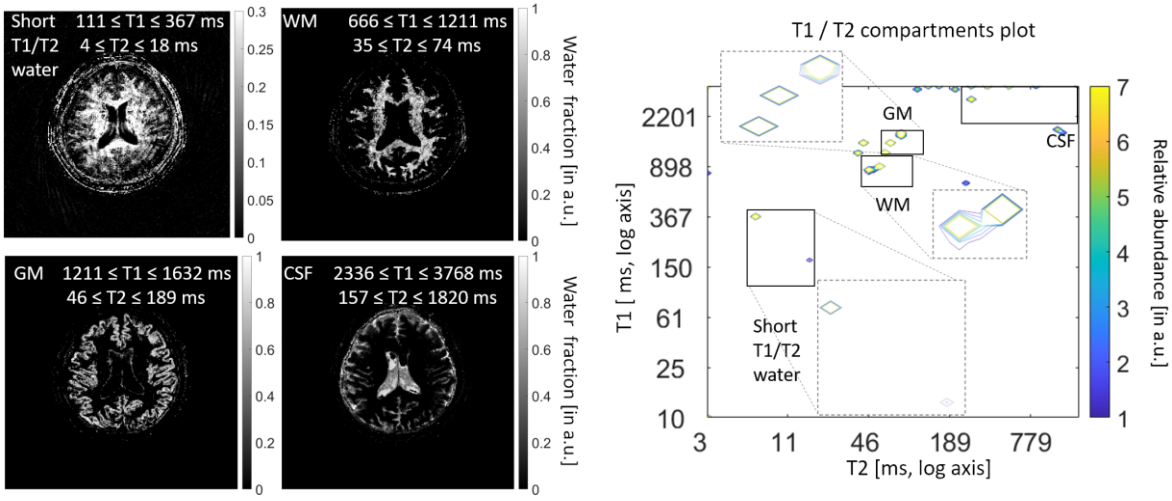

Figure 3 Multi-compartment analysis of our proposed mIR MRF for a healthy volunteer. The scan time was 24s/slice. Four-compartment brain maps were obtained from a direct pixel-wise separation. (left) The first compartment with $111 \leqslant T1 \leqslant 367$ ms and $4 \leqslant T2 \leqslant 18$ ms is considered as short T1/T2 water. (right) the T1/T2 compartments plot. Dash boxes were zoom-in views show the contours of peaks, and the peak amplitudes (as relative abundances) were color-coded. The solid boxes indicate the T1 and T2 ranges for quantifying the different water compartments. It should be noted that the water with short T1/T2 and white matter free water can be separated in the T1/T2 compartments plot. The size of marker indicted the contour of the compartment at the level of amplitude/ relative abundance $\geqslant$1.0 (in a.u.). For the contour plot, seven levels ranging from relative abundances of 1.0 to 7.0 (in a.u.) were displayed. WM: white matter; GM: grey matter; CSF: cerebrospinal fluid.

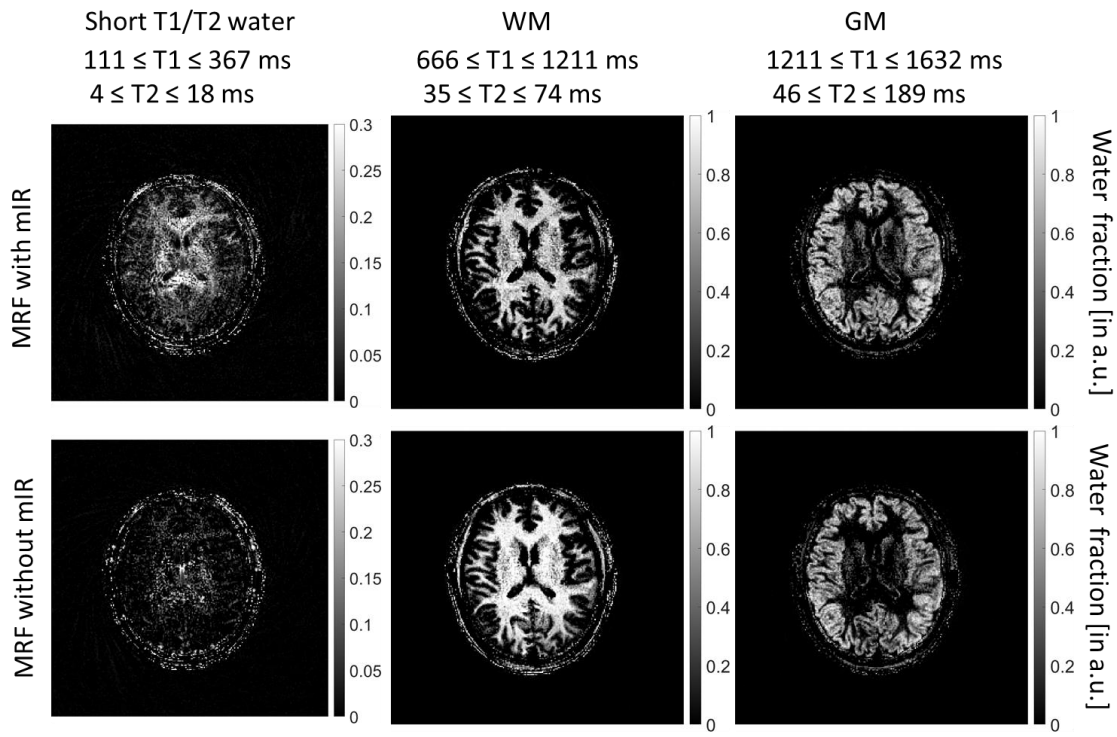

Figure 4 Multi-compartment analysis of another healthy volunteer obtained from MRF with and without the proposed mIR scheme. The use of mIR scheme clearly improved the detection of myelin water content. The scan time for both protocols was 24 s/slice.

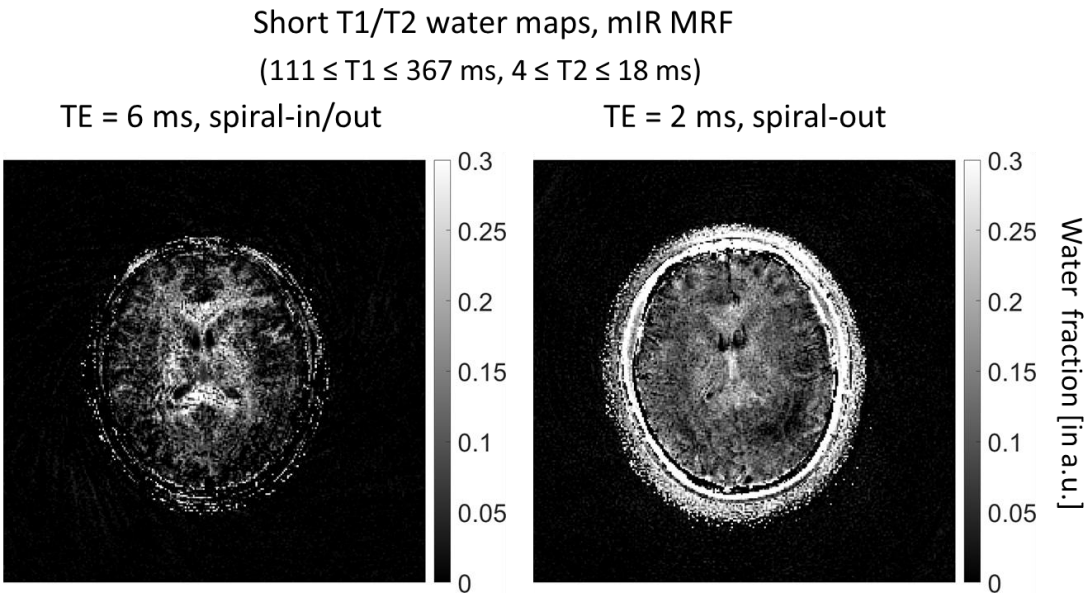

Figure 5 Multi-compartment analysis of mIR MRF with two different spiral readout trajectories, namely spiral-in/out trajectory with TE of 6 ms and spiral-out trajectory with TE of 2 ms for the same volunteer as that in Figure 3. The spiral-in/out trajectory provided a higher signal compared with the spiral-out trajectory.

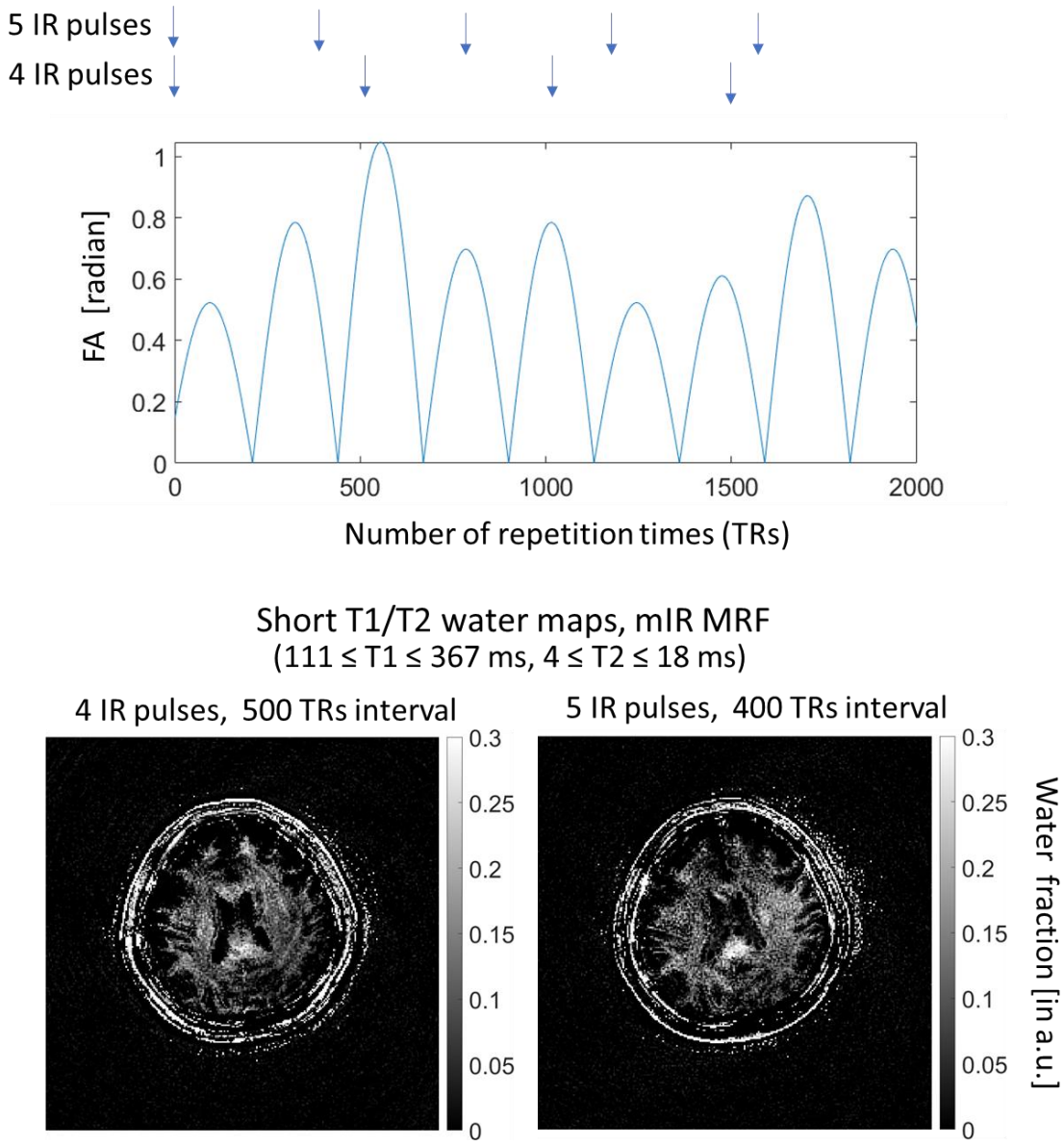

Figure 6 The comparison of the short T1/T2 water compartment mapping using our proposed mIR MRF with mIR scheme with 4 versus 5 IR's. Short T1/T2 water content can be detected using either mIR scheme. That from the 5-IR scheme had fewer artifacts.